Assignment of the Hydrogen-Out-Of-Plane and -in-Plane Vibrations of the Retinal Chromophore in the K Intermediate of *pharaonis* Phoborhodopsin†

Yuji Furutani,‡,§ Yuki Sudo,‡ Akimori Wada,|| Masayoshi Ito,|| Kazumi Shimono,⊥ Naoki Kamo,⊥ and Hideki Kandori*,‡,§

Department of Materials Science and Engineering, Nagoya Institute of Technology, Showa-ku, Nagoya 466-8555, Japan, Graduate School of Organic Chemistry for Life Science, Kobe Pharmaceutical University, Higashinada-ku, Kobe 658-8558, Japan, Laboratory of Biophysical Chemistry, Graduate School of Pharmaceutical Sciences, Hokkaido University, Sapporo 060-0812, Japan, and Core Research for Evolutional Science and Technology (CREST), Japan Science and Technology Corporation, Kyoto 606-8502, Japan

Received May 28, 2006; Revised Manuscript Received August 8, 2006

ABSTRACT: *pharaonis* phoborhodopsin (*p*pR; also called *pharaonis* sensory rhodopsin II, *p*sR-II) is a photoreceptor protein for negative phototaxis in *Natronomonas pharaonis*. Photoisomerization of the retinal chromophore from all-*trans* to 13-*cis* initiates conformational changes of the protein leading to activation of the cognate transducer protein (*p*HtrII). Elucidation of the initial photoreaction, formation of the K intermediate of *p*pR, is important for understanding the mechanism of storage of photon energy. We have reported the K minus *p*pR Fourier transform infrared (FTIR) spectra, including several vibrational bands of the retinal, the protein, and internal water molecules. It is interesting that more vibrational bands were observed in the hydrogen-out-of-plane (HOOP) region than for the light-driven proton pump, bacteriorhodopsin. This result implied that the steric constraints on the retinal chromophore in the binding pocket of *p*pR are distributed more widely upon formation of the initial intermediate. In this study, we assigned the HOOP and hydrogen-in-plane vibrations by means of low-temperature FTIR spectroscopy applied to *p*pR reconstituted with retinal deuterated at C7, C8, C10−C12, C14, and C15. As a result, the 966 (+)/971 (−) and 958 (+)/961 (−) cm^{-1} bands were assigned to the C7═C8 and C11═C12 Au HOOP modes, respectively, suggesting that the structural changes spread to the middle part of the retinal. The positive bands at 1001, 994, 987, and 979 cm^{-1} were assigned to the C15−HOOP vibrations of the K intermediate, whose frequencies are similar to those of the K_L intermediate of bacteriorhodopsin trapped at 135 K. Another positive band at 864 cm^{-1} was assigned to the C14−HOOP vibration. Relatively many positive bands of hydrogen-in-plane vibrations supported the wide distribution of structural changes of the retinal as well. These results imply that the light energy was stored mainly in the distortions around the Schiff base region while some part of the energy was transferred to the distal part of the retinal.

pharaonis phoborhodopsin (*p*pR)[1] from *Natronomonas pharaonis* is a member of the archaeal rhodopsin family [bacteriorhodopsin, halorhodopsin, sensory rhodopsin (also called sensory rhodopsin I), and phoborhodopsin (also called sensory rhodopsin II] (*1*−*4*). *p*pR is a photosensor for negative phototaxis which activates the cognate transducer protein, *p*HtrII, upon light absorption. It possesses a retinal chromophore which is connected to one of its seven-transmembrane helices, similar to the case of well-studied proton pump bacteriorhodopsin (BR) (*5*−*7*). In *p*pR and BR, the retinal forms a Schiff base linkage with Lys205 and Lys216, respectively, and the protonated Schiff base is stabilized by a negatively charged counterion, Asp75 and Asp85, respectively. Light absorption triggers *trans*−*cis* photoisomerization of the retinal chromophore at the C13═C14 position in its electronically excited state (*8*), followed by rapid formation of the ground-state species such as the K intermediate (*9*). The same process occurs in BR. Relaxation of the primary intermediates leads to the formation of late intermediates, such as ppR_L, ppR_M, ppR_N, and ppR_O. The structural changes in these intermediates eventually lead to the activation of *p*HtrII.

The initial photoreaction of BR and *p*pR is the same *trans*−*cis* isomerization, but the amount of captured energy is significantly different. It was reported that the enthalpy change of the formation of ppR_K was 88 kJ/mol (wild type) and 134 kJ/mol (*p*pR protein with a six-histidine tag for purification) (*10*). These values are larger than that for BR (55 kJ/mol) (*11*). The wavelength of light maximally absorbed by each pigment is ∼500 and ∼570 nm, respec-

† This work was supported in part by grants from Japanese Ministry of Education, Culture, Sports, Science, and Technology to H.K. (15076202) and by research fellowships from the Japan Society for the Promotion of Science for Young Scientists to Y.F.

* To whom correspondence should be addressed. Phone and fax: 81-52-735-5207. E-mail: kandori@nitech.ac.jp.

‡ Nagoya Institute of Technology.

§ Japan Science and Technology Corp.

|| Kobe Pharmaceutical University.

⊥ Hokkaido University.

[1] Abbreviations: *p*pR, *pharaonis* phoborhodopsin; ppR_K, K intermediate of *p*pR; *p*HtrII, *pharaonis* halobacterial transducer II; BR, light-adapted bacteriorhodopsin with all-*trans* retinal as a chromophore; BR_K, K intermediate of BR; BR_{KL}, K_L intermediate of BR; HOOP, hydrogen-out-of-plane; PC, L-α-phosphatidylcholine.

10.1021/bi0610597 CCC: $33.50
Published on Web 09/12/2006

tively, corresponding to energies of 239 and 210 kJ/mol, respectively. The input energy of *p*pR is 1.1 times greater than that of BR, while the amount of the captured energy is 1.6−2.4 times larger. Therefore, the difference in energy of incident light cannot account for the difference in the captured energy between *p*pR and BR. This observation may be connected to the fact that the thermal isomerization (dark adaptation) extent of BR was larger than that of *p*pR. The former has an approximately 1:1 ratio between all-*trans* and 13-*cis* forms in the dark, while the latter has almost completely all-*trans* retinal. The conclusion was that the retinal pocket of *p*pR is restricted to accommodate only all-*trans* retinal, and the *trans*−*cis* isomerization disrupts a larger number of weak interactions and/or causes larger perturbation of the protein and retinal skeleton. However, the detailed structural information about the K intermediate is necessary for establishing a better understanding of the photoisomerization.

X-ray crystallography was applied not only to the ground state of *p*pR, including the transducer-free *p*pR (*12*, *13*) and *p*pR in complex with a truncated *p*HtrII (*14*), but also to the primary intermediate, ppR$_K$, in the absence of *p*HtrII (*15*). Recently, the crystal structures of the K and M intermediates in complex with a truncated *p*HtrII were also determined (*16*). These atomic structures provide important information about light-induced structural changes of the protein moiety. However, these structural models are constructed from the diffraction data with limited resolution (>2.0 Å), and hydrogen atoms are not observable. Therefore, the retinal conformation, particularly in the intermediate state, has to be confirmed by other spectroscopic methods, such as FTIR spectroscopy.

We have reported FTIR difference spectra of ppR$_K$ in the absence (*17*−*21*) and presence of *p*HtrII (*22*, *23*). In particular, it was revealed that more hydrogen-out-of-plane (HOOP) vibrations appear upon formation of ppR$_K$ than in BR$_K$ (*19*). In the case of BR, an intense band was observed at 957 cm^{-1}, which is sensitive to deuteration of the Schiff base (*24*−*26*). FTIR spectroscopy of rhodopsins with isotope-labeled retinal is a powerful tool (*27*, *28*). By using BR samples reconstituted with C15−D retinal, the band at 957 cm^{-1} was assigned to the C15−HOOP vibration of BR$_K$ (*26*). Other HOOP vibrations have not been assigned yet, but these are smaller than the C15−HOOP vibration. In the literature, the intensity of a HOOP band correlates with a degree of retinal distortion of the corresponding position (*29*). Therefore, it was concluded that the retinal distortion in BR$_K$ was localized at the C15 position. On the other hand, eight relatively small bands were observed at 1001, 994, 987, 979, 966, 958, 945, and 864 cm^{-1} on the positive side of the ppR$_K$ minus *p*pR difference infrared spectra (*19*). Among them, the bands at 1001, 994, and 987 cm^{-1} are sensitive to deuteration of the Schiff base, which indicates that at least one of them is a candidate for the C15−HOOP vibration. However, the assignment of the HOOP bands has not been carried out, and it is difficult to reach reliable conclusions about the retinal distortion in the ppR$_K$ intermediate.

In this paper, we prepared *p*pR samples reconstituted with retinals deuterated at C7, C8, C10−C12, C14, and C15 and assigned the HOOP and hydrogen-in-plane vibrations. As a result, the 966 (+)/971 (−) and 958 (+)/961 (−) cm^{-1} bands were assigned to the C7═C8 and C11═C12 Au HOOP modes, respectively, suggesting that structural changes spread to the middle part of the retinal. The positive bands at 1001, 994, 987, and 979 cm^{-1} were assigned to the C15−HOOP vibration of the K intermediate, the frequencies of which are similar to that of the K$_L$ intermediate of bacteriorhodopsin trapped at 135 K (*30*). The other positive band at 864 cm^{-1} was assigned to the C14−HOOP vibration. Relatively many positive bands of hydrogen-in-plane vibrations supported the idea of a wide distribution of structural changes of the retinal as well. These results implied that the light energy was stored mainly in the distortions around the Schiff base region while some part of the energy was transferred to the distal part of the retinal.

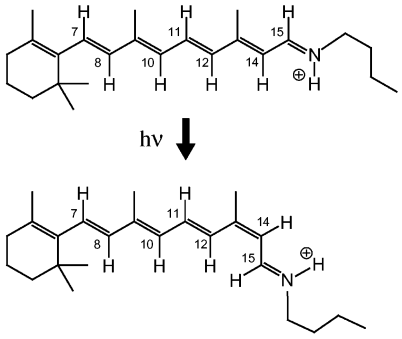

FIGURE 1: Schematic drawing of protonated all-*trans* and 13-*cis* forms of the retinal Schiff base. Hydrogen atoms indicate the positions of deuteration.

MATERIALS AND METHODS

Preparation of the ppR Samples. The *p*pR samples were prepared as described previously (*19*, *31*). Briefly, the *p*pR protein with a histidine tag at the C-terminus was expressed in *Escherichia coli*, solubilized with 1.5% *n*-dodecyl *β*-D-maltoside, and purified by Ni column chromatography. The purified *p*pR sample was then reconstituted into L-α-phosphatidylcholine (PC) liposomes by removing the detergent with Bio-beads, where the molar ratio of the added PC to *p*pR was 50:1. The *p*pR samples with retinal deuterated at C7, C8, C10−C12, C14, and C15 (Figure 1) (*32*) were produced by adding all-*trans* retinal labeled at each position (1 mM) to the *E. coli* culture instead of the unlabeled all-*trans* retinal.

FTIR Spectroscopy. FTIR spectroscopy was performed as described previously (*19*). The samples of *p*pR in PC liposomes were washed twice (2 mM phosphate buffer at pH 7.0); 90 mL of the *p*pR sample was dried on a BaF_2 window with a diameter of 18 mm. The dry film was then rehydrated by putting an ∼1 mL drop of water beside the film and sealing with another window and a silicon rubber O-ring (*19*, *21*, *33*). After hydration, the sample was placed in a cell, which was mounted in an Oxford DN-1704 cryostat placed in the Bio-Rad FTS-40 spectrometer. All spectra were measured with 2 cm^{-1} resolution. The ppR$_K$ minus *p*pR difference spectra were measured as follows (*19*). Illumination of the *p*pR film at pH 7 with 450 nm light at 77 K for 2 min converted *p*pR to ppR$_K$, and subsequent illumination with >560 nm light forced ppR$_K$ to revert to *p*pR. The difference spectrum was calculated from spectra constructed with 128 interferograms collected before and after the illumination. Twenty-four spectra obtained in this way were averaged for the ppR$_K$ minus *p*pR spectra.

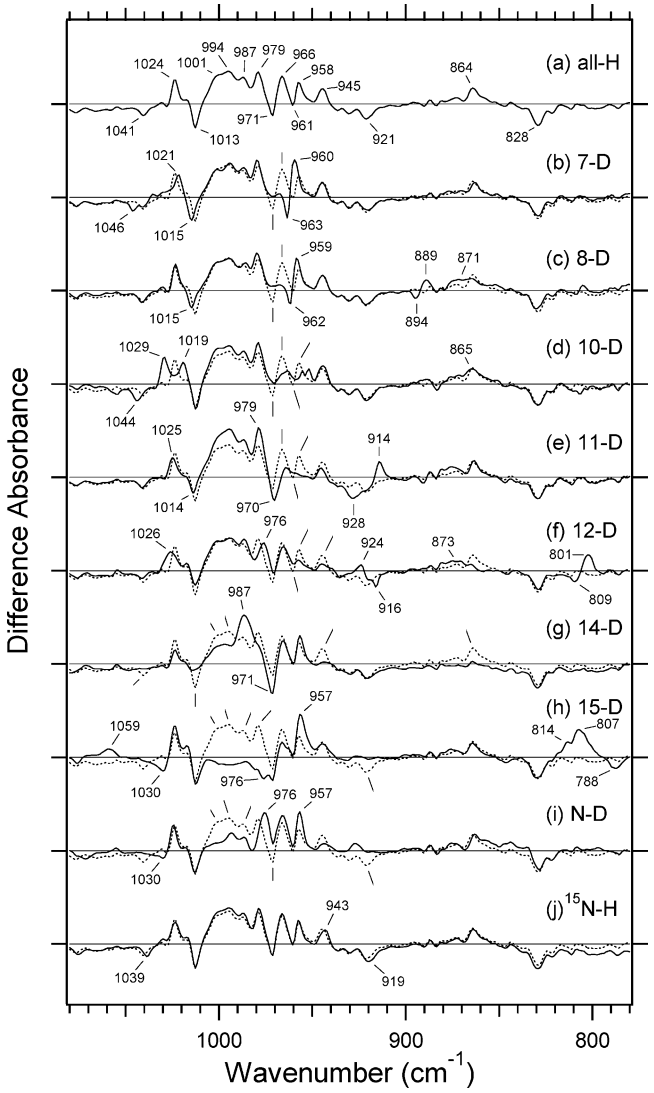

FIGURE 2: *p*R$_K$ minus *p*R difference spectra in the 1080−780 cm^{-1} region. Hydrogen-out-of-plane and methyl rocking vibrations are mainly observed in this frequency region. These spectra were recorded by using *p*R reconstituted with unlabeled retinal (a) or retinal deuterated at C7 (b), C8 (c), C10 (d), C11 (e), C12 (f), C14 (g), C15 (h), and ϵN of Lys (i). [ϵ-^{15}N]Lys-labeled *p*R was also studied (j). The solid lines of panels b−j are from the labeled samples. The dotted lines are duplicates of the spectra of panel a.

RESULTS

Hydrogen-Out-Of-Plane Vibrations of Retinal Observed in the ppR$_K$ minus ppR Difference Infrared Spectra. Figure 2 shows the *p*R$_K$ minus *p*R difference infrared spectra in the 1080−780 cm^{-1} region. Hydrogen-out-of-plane (HOOP) and methyl rocking vibrations of the retinal molecule are mainly observed in this frequency region. There are nine major positive and six negative bands in this frequency region (Figure 2a). Among them, only the 828 cm^{-1} band was not affected by deuteration of the polyene chain of the retinal, suggesting it comes from the protein moiety. The others could be assigned to HOOP or methyl rocking vibrations.

In the C7−D and C8−D spectra, the band pair at 971 (−)/966 (+) cm^{-1} disappears probably because of the isotope-induced downshift to <780 cm^{-1}, though the frequency region is below our window transmission range. It is reasonable to assign these bands to a vibrationally coupled HOOP mode (C7−H═C8−H Au HOOP). Hydrogen atoms located in trans geometry in a polyene chain can couple with each other forming an Au HOOP vibration in the 970−950 cm^{-1} range and a Bg HOOP vibration in the 850−750 cm^{-1} range (*34*). Introduction of deuterium disrupts the coupling, and each HOOP vibration is observed separately. The band pair at 894 (−)/889 (+) cm^{-1} in the C8−D spectrum can be assigned to the C7−HOOP vibration. On the other hand, we could not observe any band in the same frequency region in the C7−D spectrum, probably because of the low intensity of the C8−HOOP vibration. Similarly, a band pair at 961 (−)/958 (+) cm^{-1} disappears in the C11−D and C12−D spectra. It suggests that these bands also come from a vibrationally coupled HOOP mode (C11−H═C12−H Au HOOP). The bands at 928 (−)/914 (+) cm^{-1} in the C11−D spectrum and at 924 (+)/916 (−) cm^{-1} in the C12−D spectrum can be assigned to the uncoupled C12−HOOP and C11−HOOP vibrations, respectively. In the C12−D spectrum, we could see the C12−DOOP (deuterium-out-of-plane) vibration at 809 (−)/801 (+) cm^{-1}.

Thus, isotope labeling at C7−H, C8−H, C11−H, and C12−H positions made it possible to assign the bands at 971 (−)/966 (+) and 961 (−)/958 (+) cm^{-1} to C7−H═C8−H and C11−H═C12−H Au HOOP modes, respectively. It should be noted that both of them are strongly affected by deuteration at the C10−H position. In the case of BR, these modes couple weakly or not at all with the C10−HOOP mode, which was assigned to the 898 cm^{-1} band in the previous Raman spectra (*35*). This result suggests that the C10−HOOP mode of *p*pR exists in the 970−950 cm^{-1} region and/or couples with the C7−H═C8−H and C11−H═C12−H Au HOOP modes.

The positive band at 864 cm^{-1} disappears in the C14−D spectrum and is slightly affected by deuteration at C12−H. This band can be assigned to the C14−HOOP mode of *p*pR$_K$, even though it is located at a frequency 33 cm^{-1} higher than that of the 13-*cis* retinal (831 cm^{-1}) (*36*) and is closer to that of the all-*trans* retinal (876 cm^{-1}) (*34*). This suggests that the chromophore of *p*pR$_K$ is in the unrelaxed 13-*cis* configuration. The corresponding negative band probably has a low intensity and could not be observed. The band at 945 cm^{-1} was also affected by deuteration at the C14−H group, which comes from the other vibration coupled with the C14−HOOP mode. Its origin has not been found yet, but it is located near the Schiff base because of the slight downshift in the ^{15}N−H spectrum.

The negative band at 921 cm^{-1} downshifts to 788 cm^{-1} in the C15−D spectrum and disappears in the N−D spectrum. [ϵ-^{15}N]Lys labeling causes its slight downshift to 919 cm^{-1}. These observations support the assignment of the 921 cm^{-1} band to the C15−H and N−H coupled HOOP mode. This assignment is almost the same as in the case of BR whose C15−H and N−H coupled HOOP vibration is located at 914 cm^{-1} (*37*). On the other hand, the assignment of the C15−HOOP vibration of the K intermediate is different. The positive bands at 994, 987, and 979 cm^{-1} and a shoulder at 1001 cm^{-1} completely disappear upon deuteration of the C15−H group and reduce their intensity in the C14−D and N−D spectra. Therefore, these bands can be assigned to the C15−H and N−H coupled HOOP vibration. It is obvious that the bands at 814 and 807 cm^{-1} correspond to the C15−DOOP mode. In the case of BR, the

C15−HOOP vibration was assigned to a strong single band at 957 cm^{-1} (*26*), in clear contrast to *p*pR.

There are also methyl rocking vibrations of the retinal polyene chain in this frequency region. The bands at 1024 (+)/1013 (−) cm^{-1} can be assigned to symmetric rocking vibrations of methyl groups connected to the C9 and C13 atoms, because of the coupling of each band with C−H vibrations in the polyene chain. It suggests that the effects of deuteration at C7−H, C8−H, C11−H, C12−H, C15−H, and Lys-ϵN-H are smaller than those at C10−H and C14−H, which are located at a position *trans* from each methyl group. However, each deuteration influences the 1024 and 1013 cm^{-1} bands differently. The negative band at 1013 cm^{-1} is not affected by deuteration at C10−H, but its intensity is reduced upon deuteration at C14−H. This suggests that the retinal methyl rocking vibration in the ground state of *p*pR mainly couples with the vibration involving the C14−H bond. On the other hand, the positive band at 1024 cm^{-1} splits into two bands at 1029 and 1019 cm^{-1} in the C10−D spectrum, and its intensity is reduced upon deuteration at C14−H. The effect of deuteration at C14−H is weaker than that seen on the negative band at 1013 cm^{-1}. It suggests that the methyl rocking vibration of the *p*pR_K intermediate mainly couples with the vibration involving the C10−H bond. The photoisomerization at the C13═C14 position probably changes the behavior of vibrational coupling of the C13−methyl and C14−H groups, because their geometry is altered from *trans* to *cis* after the isomerization. In the case of the ground state of BR, a strong Raman band at 1008 cm^{-1} was observed (*35*) and the deuteration effect is similar to that of *p*pR. However, there is no information about the effect of deuteration at C10−H and C14−H for the methyl rocking vibration of the K intermediate of BR. The dark-adapted BR which also has 13-*cis* retinal but 15-*syn* geometry exhibits a strong Raman band at 1012 cm^{-1}, the intensity of which was reduced upon deuteration at C14−H and C10,-C11−H (*38*). Therefore, the behavior of the methyl rocking vibration upon deuteration at the polyene chain of *p*pR is similar to that of BR, while the band behavior of *p*pR_K is somewhat different from that of the dark-adapted BR.

The negative band at 1041 cm^{-1} is also affected by deuteration. It exhibits a small downshift upon [ϵ-^{15}N]Lys labeling, suggesting it originates from the vibration involving the Schiff base nitrogen. The most probable candidate is the C−N stretching vibration of Lys205. The corresponding band of *p*pR_K was not observed, but there is a positive band at 1059 cm^{-1} in the C15−D spectra. The C−N stretching mode in *p*pR_K may be coupled with the vibration including the C15−H bond and upshifts to more than 1080 cm^{-1}.

Hydrogen-In-Plane Vibrations of the Retinal Observed in the ppR_K minus ppR Difference Infrared Spectra. The hydrogen-in-plane vibrations of the retinal can also be assigned by using the deuterated retinals. Figure 3 shows the *p*pR_K minus *p*pR spectra in the 1430−1270 cm^{-1} region. Six positive major bands and one negative major band were observed in this frequency region. Relatively many bands observed on the positive side are due to the decrease in symmetry at the *cis* bend described in the literature (*36*). The replacement of each hydrogen atom in the polyene chain of the retinal with deuterium induces an ~400 cm^{-1} downshift of the hydrogen-in-plane vibrations, resulting in the appearance of the corresponding deuterium-in-plane vibration in the HOOP region.

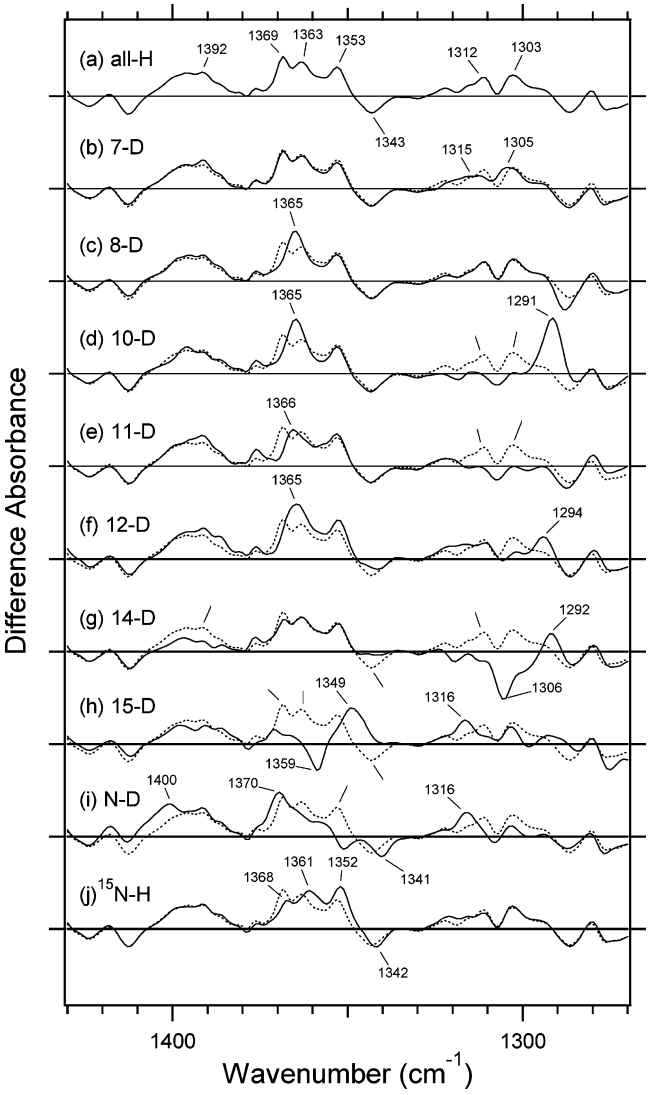

FIGURE 3: *p*pR_K minus *p*pR difference spectra in the 1430−1270 cm^{-1} region. Hydrogen-in-plane vibrations are mainly observed in this frequency region. These spectra were recorded by using *p*pR reconstituted with unlabeled retinal (a) or retinal deuterated at C7 (b), C8 (c), C10 (d), C11 (e), C12 (f), C14 (g), C15 (h), and ϵN of Lys (i). [ϵ-^{15}N]Lys-labeled *p*pR was also studied (j). The solid lines of panels b−j are from the labeled samples. The dotted lines are duplicates of the spectra of panel a.

The positive bands at 1312 and 1303 cm^{-1} completely disappear in the C10−D and C11−D spectra, suggesting that these bands originate from the C10−H and C11−H in-plane vibrations of *p*pR_K. The corresponding C11−D in-plane vibration appears at 979 (+)/970 (−) cm^{-1}, while the C10−D in-plane vibration is not detected. The absence of the C11−H and C10−H in-plane vibrations of *p*pR can probably be explained by their intensity being lower than that in *p*pR_K. The intense positive band at 1291 cm^{-1} can be assigned to the C8−C9 stretching vibration of *p*pR_K which is not seen in the unlabeled spectra. The upshift of the C8−C9 stretch is caused by decoupling from the C10−H in-plane vibration. The two positive bands exhibit different isotope effects when other hydrogens are deuterated. The 1312 cm^{-1} band disappears in the C14−D spectrum and is upshifted in the C15−D and N−D spectra, while the 1303 cm^{-1} band is downshifted in the C12−D and C14−D spectra. Both bands

Table 1: Assignments of HOOP and Hydrogen-In-Plane Vibrations of *p*pR and *p*pR$_K$

*p*pR	*p*pR$_K$	BR[a,b]	BR$_K$[c]	BR$_{KL}$[d]	BR$_L$[b]	all-*trans* retinal[e]	13-*cis* retinal[f]	assignments
971	966	985	–	–	–	966	967	C7−H═C8−H Au HOOP
961	958	959	–	–	–	959	955	C11−H═C12−H Au HOOP
–	864	842	–	–	–	876	831	C14−HOOP
921	1001, 994, 987, 979	911	957	985, 977, 966, 957	1073, 1064, 1056	–	–	C15−HOOP
–	1312, 1303	1330	–	–	–	–	1348	C10−H in-plane
–	1312, 1303	1322	–	–	–	1279, 1270	1273	C11−H in-plane
1343	1392	1345	–	–	–	1334	1348	C14−H in-plane
–	1369, 1363	1345	–	–	–	1334	1399	C15−H in-plane
–	1353	1348	1348	1354	1400	–	–	N−H in-plane

[a] From ref *35*. [b] From ref *37*. [c] From ref *26*. [d] From ref *30*. [e] From ref *34*. [f] From ref *36*.

are upshifted in the C7−D spectrum. These complicated isotope effects probably reflect the specific property of the retinal binding site in *p*pR, because the corresponding C11−H in-plane vibration of 13-*cis* retinal observed at 1273 cm^{-1} in organic solvent was not affected by deuteration at C12−H and C15−H (*36*).

Upon deuteration at C14−H, the positive band at 1392 cm^{-1} undergoes a reduction in intensity and the negative band at 1343 cm^{-1} disappears. The former and the latter band can be assigned to the C14−H in-plane vibrations of *p*pR$_K$ and *p*pR, respectively. The corresponding C14−D in-plane vibrations were detected at 987 (+)/971 (−) cm^{-1}. The difference in frequency between the C14−H in-plane vibrations of *p*pR$_K$ and *p*pR is 49 cm^{-1}, while that of the C14−D in-plane vibrations is 16 cm^{-1}. It is probably explained by decoupling of the C14−D in-plane vibration from other C−C stretching or C−H in-plane vibrations. The band at 1306 cm^{-1} is a decoupled C12−C13 stretch, similar to the assignment for BR (*35*).

The positive bands at 1369 and 1363 cm^{-1} disappear, and the bands at 1353 (+)/1343 (−) cm^{-1} shift to 1349 (+)/1359 (−) cm^{-1} in the C15−D spectra. The 1369 and 1363 cm^{-1} bands can be assigned to the C15−H in-plane vibration of *p*pR$_K$, while the bands at 1353 (+)/1343 (−) cm^{-1} originate from other vibrations. The negative band at 1343 cm^{-1} was already assigned to the C14−H in-plane vibration, and the upshift implies that it couples with the vibration, including the motion of C15−D. The positive band at 1353 cm^{-1} can be assigned to the N−H in-plane vibration because of its disappearance from the N−D spectrum.

The bands at 1369 (+) and 1363 (+), 1353 (+), and 1343 (−) cm^{-1} have been assigned to the C15−H, N−H, and C14−H in-plane vibrations, respectively. These assignments are also supported by the downshifts seen in the ^{15}N−H spectrum, suggesting their origin from the vicinity of the Schiff base. The positive bands at 1369 and 1363 cm^{-1} are also affected by deuteration at C8 and C10−C12 and are combined to one positive band around at 1365 cm^{-1}. It implies that the C15−H in-plane vibration couples with C8−H, C10−H, C11−H, and C12−H motions, probably with their in-plane vibrations.

DISCUSSION

The HOOP and hydrogen-in-plane vibrations of the retinal in *p*pR and *p*pR$_K$ were assigned by using the *p*pR samples reconstituted with various deuterated retinals. The results are listed in Table 1. The assignments for BR and all-*trans* and 13-*cis* retinal in organic solvent are also presented for comparison. It should be noted that the lipid composition for the *p*pR samples (PC) is different from that for BR in purple membranes, which comprises several polar lipids, such as phosphatidylglycerophosphate methyl ester (PGP-Me) and phosphatidylglycerol (PG). Such a difference may affect vibrational bands. However, the present *p*pR$_K$ minus *p*pR spectra in PC liposomes are very similar to those published by Hein et al. (*39*), where the *p*pR samples were reconstituted into the purple membrane lipids. It is thus likely that the early step of the photocyle is not essentially affected by the difference in lipid composition.

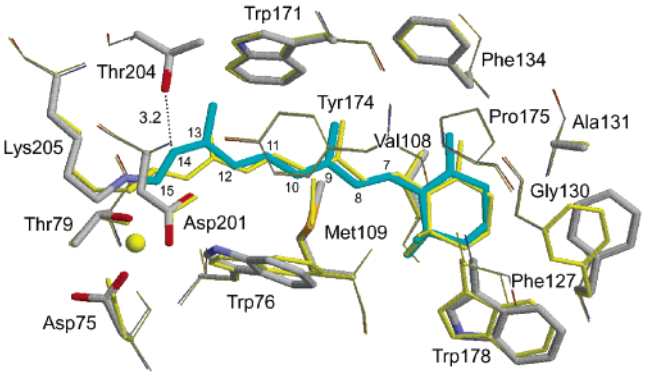

FIGURE 4: X-ray crystal structures of the K intermediate (colored CPK) and *p*pR (colored yellow). Amino acid residues within 5.0 Å of the retinal molecule are shown. The yellow sphere is a water molecule bridging the Schiff base and Asp75. The coordinates were obtained from the Protein Data Bank (entry 1GU8) (*15*).

Vibrational changes in the C7−H═C8−H and C11−H═C12−H Au HOOP modes upon formation of *p*pR$_K$ suggest that photoisomerization from all-*trans* to 13-*cis* retinal causes conformational changes in the retinal in these regions. The intensities of the positive bands at 966 and 958 cm^{-1} are somewhat larger than those of the negative bands at 971 and 961 cm^{-1}, suggesting a slight increase in the level of distortion at C6−C7, C8−C9, C10−C11, and C12−C13 single bonds. However, since the frequencies are very similar to those of BR and all-*trans* and 13-*cis* retinal, the conformation of these regions should not be very different from that of the ordinary retinal. This result can be explained by the change in interaction between the retinal and the protein moiety upon photoisomerization. According to the crystal structure (*15*), the C7, C8, C10, and C11 atoms are displaced ~0.3−0.5 Å from their original positions toward the Schiff base (Figure 4). The electrostatic field at the new positions induces a different dipolar moment in the retinal molecule, resulting in intensity changes of the C7−H═C8−H and C11−H═C12−H Au HOOP modes. Such movement was

not observed in the crystal structure of the K intermediate of BR (*40*−*42*), so these HOOP modes have not been detected in the BR_K minus BR spectra. Edman et al. reported that the structural reason for the different movement of the retinal is explained by the replacement of Met145 in BR with Phe134 in *p*pR (*15*). Namely, it was proposed that Met145 is in a tight contact with the C5 methyl group of the β-ionone ring and inhibits any movement of this group upon photoisomerization in BR.

One of the most prominent differences in the HOOP region between BR_K and *p*pR_K is in the C15−HOOP mode. The former has an intense band at 957 cm^{-1}, and the latter has broad and multiple bands at 1001, 994, 987, and 979 cm^{-1}. It was suggested that the intense C15−HOOP mode comes from the increased degree of polarization of the C15−H bond due to the out-of-plane twist of the C═N bond of the Schiff base. Therefore, the result that the intensity of the C15−HOOP mode of *p*pR_K is lower than that of BR_K suggests that the twist of the C═N bond of the Schiff base is already partially relaxed in *p*pR_K. It probably correlates with the observation of the larger electron density difference around the side chain of Lys205 in the crystal structure of *p*pR_K. That is, the relaxation of the C═N bond induces distortion of the side chain of Lys205. Moreover, not only the intensity but also the frequency is different between BR_K and *p*pR_K. The center of the C15−HOOP band of *p*pR_K is located at 994 cm^{-1}, whereas that of BR_K is located at 957 cm^{-1}. It should be noted that the spectral features of the C15−HOOP mode of *p*pR_K are rather similar to those of BR_{KL} which is observed at 985 cm^{-1} (*30*). In addition to the similarity of the N−H hydrogen-in-plane vibration (1353 cm^{-1} in *p*pR_K and 1354 cm^{-1} in BR_{KL}), the Schiff base C═N configuration and its environment of *p*pR_K may resemble those of BR_{KL}. However, the effect of deuteration of the Schiff base is somewhat different. The C15−HOOP band in BR_{KL} is slightly downshifted from 985 to 980 cm^{-1}, while in the case of *p*pR, the C15−HOOP band is downshifted from 994 to 976 cm^{-1}. In the former, the difference in frequency is 5 cm^{-1}, while in the latter, it is 18 cm^{-1}. Because the frequency difference accounts for the degree of vibrational coupling, the Schiff base N−HOOP and C15−HOOP vibrations of *p*pR_K couple more strongly than those of BR_{KL}.

The other significant result is the identification of the C14−HOOP and C14 hydrogen-in-plane vibrations. We previously reported the existence of steric constraint in the C14−H bond, proven by the observation of increased intensity of the C14−D stretching vibration at 2244 cm^{-1} upon retinal photoisomerization (*17*). The effect was also confirmed in this work by the observation of the C14−HOOP and C14 hydrogen in-plane vibrations at frequencies relatively higher than those for 13-*cis* retinal. According to the literature, the presence of a large dipole in the ground state causes an increase in infrared absorption if no symmetry restrictions are assumed (*29*). Therefore, the relatively intense C14−D stretching, C14−HOOP, and C14 hydrogen-in-plane vibrations in the *p*pR_K intermediate should be interpreted as an indication of electric polarization of the C14−H bond. It may be caused by formation of weak interaction with Thr204, whose hydroxyl oxygen is 3.2 Å from the C14 atom in *p*pR_K (Figure 4). It is interesting that the structural changes in the hydrogen bond of Thr204 upon photoisomerization are different (*22*, *23*), while the molecular structures of *p*pR alone and *p*pR in complex with *p*HtrII are very similar, especially in the retinal binding pocket (*14*, *16*). Future studies will provide a better understanding by focusing on the effect of Thr204 on the light-induced structural changes of *p*pR in the absence and presence of *p*HtrII.

The previous studies by opto-acoustic spectroscopy revealed that the enthalpy change upon the formation of the K intermediate of *p*pR is larger than that for BR (*10*). The former value is 142 or 88 kJ/mol with or without six-His tag, respectively, while the latter value is 55 kJ/mol. It may originate from the difference in the degree of structural change around the retinal. We detected the environmental change in the middle of the retinal polyene chain by identifying the C7═C8 and C11═C12 Au HOOP modes and C10 and C11 hydrogen in-plane vibrations. X-ray crystallography also revealed that the retinal isomerization causes displacement of the β-ionone ring (Figure 4). Both characteristic features were not observed upon the formation of the BR_K intermediate (*40*−*42*). While such structural change is clearly observed by X-ray crystallography, it is difficult to notice the existence of a steric constraint at the C14−H bond. In this work, we for the first time succeeded in identifying C14−HOOP and C14 hydrogen-in-plane vibrations of *p*pR_K by means of FTIR spectroscopy with retinals deuterated at each position of a polyene chain. In addition to the previous report of the intense C14−D stretching vibration of *p*pR_K (*17*), the result presented here suggests that some part of photon energy is captured in the distortion of C14−H bond. In the presence of *p*HtrII, a part of the stored energy may be utilized to activate the rearrangement of Thr204, resulting in the formation of a very strong hydrogen bond. Such energy differences were reported by the time-resolved transient grating (TG) method as well, where the enthalpy changes of the L intermediate of *p*pR are estimated to be 170 kJ/mol for transducer-free *p*pR and 80 kJ/mol for *p*pR connected with *p*HtrII (*43*). This observation is in clear contrast to the case of BR, where structural changes upon retinal isomerization are mainly limited in the Schiff base region (*40*−*42*). Considerable weakening of hydrogen bonds of the Schiff base N−H group (*44*) and several water molecules (*5*, *45*−*47*) and distortion of the retinal molecule probably account for almost all of the stored energy. According to the recent theoretical calculation, the total energy captured in BR_K is calculated to be 67 kJ/mol and the contribution of hydrogen bonds is estimated to be 46 kJ/mol (69%) (*48*, *49*). The hydrogen bonding alterations of the Schiff base and water molecules in *p*pR are similar to those of BR (*21*). Therefore, the excess energy storage may be achieved by larger structural changes around the β-ionone ring and the C14−H distortion.

ACKNOWLEDGMENT

We thank Prof. Leonid S. Brown for critical reading of our manuscript.

REFERENCES

1. Kamo, N., Shimono, K., Iwamoto, M., and Sudo, Y. (2001) Photochemistry and photoinduced proton-transfer by *pharaonis* phoborhodopsin, *Biochemistry (Moscow) 66*, 1277−1282.
2. Sasaki, J., and Spudich, J. L. (2000) Proton transport by sensory rhodopsins and its modulation by transducer-binding, *Biochim. Biophys. Acta 1460*, 230−239.

3. Sudo, Y., Kandori, H., and Kamo, N. (2004) Molecular mechanism of protein-protein interaction of *pharaonis* phoborhodopsin/transducer and photo-signal transfer reaction by the complex, *Recent Res. Dev. Biophys. 3*, 1−16.
4. Klare, J. P., Bordignon, E., Engelhard, M., and Steinhoff, H. J. (2004) Sensory rhodopsin II and bacteriorhodopsin: Light activated helix F movement, *Photochem. Photobiol. Sci. 3*, 543−547.
5. Kandori, H. (2000) Role of internal water molecules in bacteriorhodopsin, *Biochim. Biophys. Acta 1460*, 177−191.
6. Lanyi, J. K. (2004) Bacteriorhodopsin, *Annu. Rev. Physiol. 66*, 665−688.
7. Neutze, R., Pebay-Peyroula, E., Edman, K., Royant, A., Navarro, J., and Landau, E. M. (2002) Bacteriorhodopsin: A high-resolution structural view of vectorial proton transport, *Biochim. Biophys. Acta 1565*, 144−167.
8. Kandori, H., Tomioka, H., and Sasabe, H. (2002) Excited-State Dynamics of *pharaonis* Phoborhodopsin Probed by Femtosecond Fluorescence Spectroscopy, *J. Phys. Chem. A 106*, 2091−2095.
9. Lutz, I., Sieg, A., Wegener, A. A., Engelhard, M., Boche, I., Otsuka, M., Oesterhelt, D., Wachtveitl, J., and Zinth, W. (2001) Primary reactions of sensory rhodopsins, *Proc. Natl. Acad. Sci. U.S.A. 98*, 962−967.
10. Losi, A., Wegener, A. A., Engelhard, M., Gartner, W., and Braslavsky, S. E. (1999) Time-resolved absorption and photothermal measurements with recombinant sensory rhodopsin II from *Natronobacterium pharaonis*, *Biophys. J. 77*, 3277−3286.
11. Zhang, D., and Mauzerall, D. (1996) Volume and enthalpy changes in the early steps of bacteriorhodopsin photocycle studied by time-resolved photoacoustics, *Biophys. J. 71*, 381−388.
12. Luecke, H., Schobert, B., Lanyi, J. K., Spudich, E. N., and Spudich, J. L. (2001) Crystal structure of sensory rhodopsin II at 2.4 angstroms: Insights into color tuning and transducer interaction, *Science 293*, 1499−1503.
13. Royant, A., Nollert, P., Edman, K., Neutze, R., Landau, E. M., Pebay-Peyroula, E., and Navarro, J. (2001) X-ray structure of sensory rhodopsin II at 2.1-Å resolution, *Proc. Natl. Acad. Sci. U.S.A. 98*, 10131−10136.
14. Gordeliy, V. I., Labahn, J., Moukhametzianov, R., Efremov, R., Granzin, J., Schlesinger, R., Buldt, G., Savopol, T., Scheidig, A. J., Klare, J. P., and Engelhard, M. (2002) Molecular basis of transmembrane signalling by sensory rhodopsin II-transducer complex, *Nature 419*, 484−487.
15. Edman, K., Royant, A., Nollert, P., Maxwell, C. A., Pebay-Peyroula, E., Navarro, J., Neutze, R., and Landau, E. M. (2002) Early structural rearrangements in the photocycle of an integral membrane sensory receptor, *Structure 10*, 473−482.
16. Moukhametzianov, R., Klare, J. P., Efremov, R., Baeken, C., Goppner, A., Labahn, J., Engelhard, M., Buldt, G., and Gordeliy, V. I. (2006) Development of the signal in sensory rhodopsin and its transfer to the cognate transducer, *Nature 440*, 115−119.
17. Sudo, Y., Furutani, Y., Wada, A., Ito, M., Kamo, N., and Kandori, H. (2005) Steric constraint in the primary photoproduct of an archaeal rhodopsin from regiospecific perturbation of C-D stretching vibration of the retinyl chromophore, *J. Am. Chem. Soc. 127*, 16036−16037.
18. Shimono, K., Furutani, Y., Kamo, N., and Kandori, H. (2003) Vibrational modes of the protonated Schiff base in *pharaonis* phoborhodopsin, *Biochemistry 42*, 7801−7806.
19. Kandori, H., Shimono, K., Sudo, Y., Iwamoto, M., Shichida, Y., and Kamo, N. (2001) Structural changes of *pharaonis* phoborhodopsin upon photoisomerization of the retinal chromophore: Infrared spectral comparison with bacteriorhodopsin, *Biochemistry 40*, 9238−9246.
20. Kandori, H., Shimono, K., Shichida, Y., and Kamo, N. (2002) Interaction of Asn105 with the retinal chromophore during photoisomerization of *pharaonis* phoborhodopsin, *Biochemistry 41*, 4554−4559.
21. Kandori, H., Furutani, Y., Shimono, K., Shichida, Y., and Kamo, N. (2001) Internal water molecules of *pharaonis* phoborhodopsin studied by low-temperature infrared spectroscopy, *Biochemistry 40*, 15693−15698.
22. Sudo, Y., Furutani, Y., Shimono, K., Kamo, N., and Kandori, H. (2003) Hydrogen bonding alteration of Thr-204 in the complex between *pharaonis* phoborhodopsin and its transducer protein, *Biochemistry 42*, 14166−14172.
23. Furutani, Y., Sudo, Y., Kamo, N., and Kandori, H. (2003) FTIR spectroscopy of the complex between *pharaonis* phoborhodopsin and its transducer protein, *Biochemistry 42*, 4837−4842.
24. Siebert, F., and Mantele, W. (1983) Investigation of the primary photochemistry of bacteriorhodopsin by low-temperature Fourier-transform infrared spectroscopy, *Eur. J. Biochem. 130*, 565−573.
25. Braiman, M., and Mathies, R. (1982) Resonance Raman spectra of bacteriorhodopsin's primary photoproduct: Evidence for a distorted 13-*cis* retinal chromophore, *Proc. Natl. Acad. Sci. U.S.A. 79*, 403−407.
26. Maeda, A., Sasaki, J., Pfefferle, J. M., Shichida, Y., and Yoshizawa, T. (1991) Fourier transform infrared spectral studies on the schiff base mode of all-*trans* bacteriorhodopsin and its photointermediates, K and L, *Photochem. Photobiol. 54*, 911−921.
27. Bagley, K., Dollinger, G., Eisenstein, L., Singh, A. K., and Zimanyi, L. (1982) Fourier transform infrared difference spectroscopy of bacteriorhodopsin and its photoproducts, *Proc. Natl. Acad. Sci. U.S.A. 79*, 4972−4976.
28. Gerwert, K., and Siebert, F. (1986) Evidence for light-induced 13-cis, 14-s-cis isomerization in bacteriorhodopsin obtained by FTIR difference spectroscopy using isotopically labelled retinals, *EMBO J. 5*, 805−811.
29. Gat, Y., Grossjean, M., Pinevsky, I., Takei, H., Rothman, Z., Sigrist, H., Lewis, A., and Sheves, M. (1992) Participation of bacteriorhodopsin active-site lysine backbone in vibrations associated with retinal photochemistry, *Proc. Natl. Acad. Sci. U.S.A. 89*, 2434−2438.
30. Maeda, A., Verhoeven, M. A., Lugtenburg, J., Gennis, R. B., Balashov, S. P., and Ebrey, T. G. (2004) Water Rearrangement around the Schiff Base in the Late K (K_L) Intermediate of the Bacteriorhodopsin Photocycle, *J. Phys. Chem. B 108*, 1096−1101.
31. Shimono, K., Iwamoto, M., Sumi, M., and Kamo, N. (1997) Functional expression of *pharaonis* phoborhodopsin in *Escherichia coli*, *FEBS Lett. 420*, 54−56.
32. Hirano, T., Fujioka, N., Imai, H., Kandori, H., Wada, A., Ito, M., and Shichida, Y. (2006) Assignment of the vibrational modes of the chromophores of iodopsin and bathoiodopsin: Low-temperature fourier transform infrared spectroscopy of ^{13}C- and ^{2}H-labeled iodopsins, *Biochemistry 45*, 1285−1294.
33. Kandori, H., and Maeda, A. (1995) FTIR spectroscopy reveals microscopic structural changes of the protein around the rhodopsin chromophore upon photoisomerization, *Biochemistry 34*, 14220−14229.
34. Curry, B., Broek, A., Lugtenburg, J., and Mathies, R. (1982) Vibrational Analysis of all-*trans*-Retinal, *J. Am. Chem. Soc. 104*, 5274−5286.
35. Smith, S. O., Braiman, M. S., Myers, A. B., Pardoen, J. A., Courtin, J. M. L., Winkel, C., Lugtenburg, J., and Mathies, R. A. (1987) Vibrational analysis of the all-*trans*-retinal chromophore in light-adapted bacteriorhodopsin, *J. Am. Chem. Soc. 109*, 3108−3125.
36. Curry, B., Palings, I., Broek, A., Pardoen, J. A., Mulder, P. P. J., Lugtenburg, J., and Mathies, R. (1984) Vibrational Analysis of 13-*cis*-Retinal, *J. Phys. Chem. 88*, 688−702.
37. Maeda, A., Balashov, S. P., Lugtenburg, J., Verhoeven, M. A., Herzfeld, J., Belenky, M., Gennis, R. B., Tomson, F. L., and Ebrey, T. G. (2002) Interaction of internal water molecules with the schiff base in the L intermediate of the bacteriorhodopsin photocycle, *Biochemistry 41*, 3803−3809.
38. Smith, S. O., Pardoen, J. A., Lugtenburg, J., and Mathies, R. (1987) Vibrational Analysis of the 13-*cis*-Retinal Chromophore in Dark-Adapted Bacteriorhodopsin, *J. Phys. Chem. 91*, 804−819.
39. Hein, M., Wegener, A. A., Engelhard, M., and Siebert, F. (2003) Time-resolved FTIR studies of sensory rhodopsin II (NpSRII) from *Natronobacterium pharaonis*: Implications for proton transport and receptor activation, *Biophys. J. 84*, 1208−1217.
40. Edman, K., Nollert, P., Royant, A., Belrhali, H., Pebay-Peyroula, E., Hajdu, J., Neutze, R., and Landau, E. M. (1999) High-resolution X-ray structure of an early intermediate in the bacteriorhodopsin photocycle, *Nature 401*, 822−826.
41. Matsui, Y., Sakai, K., Murakami, M., Shiro, Y., Adachi, S., Okumura, H., and Kouyama, T. (2002) Specific damage induced by X-ray radiation and structural changes in the primary photoreaction of bacteriorhodopsin, *J. Mol. Biol. 324*, 469−481.
42. Schobert, B., Cupp-Vickery, J., Hornak, V., Smith, S., and Lanyi, J. (2002) Crystallographic structure of the K intermediate of bacteriorhodopsin: Conservation of free energy after photoisomerization of the retinal, *J. Mol. Biol. 321*, 715−726.

43. Inoue, K., Sasaki, J., Morisaki, M., Tokunaga, F., and Terazima, M. (2004) Time-resolved detection of sensory rhodopsin II-transducer interaction, *Biophys. J. 87*, 2587−2597.
44. Kandori, H., Belenky, M., and Herzfeld, J. (2002) Vibrational frequency and dipolar orientation of the protonated Schiff base in bacteriorhodopsin before and after photoisomerization, *Biochemistry 41*, 6026−6031.
45. Shibata, M., Tanimoto, T., and Kandori, H. (2003) Water molecules in the Schiff base region of bacteriorhodopsin, *J. Am. Chem. Soc. 125*, 13312−13313.
46. Shibata, M., and Kandori, H. (2005) FTIR studies of internal water molecules in the Schiff base region of bacteriorhodopsin, *Biochemistry 44*, 7406−7413.
47. Garczarek, F., and Gerwert, K. (2006) Functional waters in intraprotein proton transfer monitored by FTIR difference spectroscopy, *Nature 439*, 109−112.
48. Hayashi, S., Tajkhorshid, E., and Schulten, K. (2002) Structural changes during the formation of early intermediates in the bacteriorhodopsin photocycle, *Biophys. J. 83*, 1281−1297.
49. Hayashi, S., Tajkhorshid, E., Kandori, H., and Schulten, K. (2004) Role of hydrogen-bond network in energy storage of bacteriorhodopsin's light-driven proton pump revealed by ab initio normal-mode analysis, *J. Am. Chem. Soc. 126*, 10516−10517.

BI0610597